Front. Struct. Civ. Eng. 2021, 15(2): 490–505
https://doi.org/10.1007/s11709-020-0669-5

RESEARCH ARTICLE

Application of machine learning algorithms for the evaluation of seismic soil liquefaction potential

Mahmood AHMAD[a,b], Xiao-Wei TANG[a], Jiang-Nan QIU[c*], Feezan AHMAD[d], Wen-Jing GU[c]

[a] *State Key Laboratory of Coastal and Offshore Engineering, Dalian University of Technology, Dalian 116024, China*

[b] *Department of Civil Engineering, University of Engineering and Technology Peshawar (Bannu Campus), Bannu 28100, Pakistan*

[c] *School of Economics & Management, Dalian University of Technology, Dalian 116024, China*

[d] *Department of Civil Engineering, Abasyn University, Peshawar 25000, Pakistan*

[*] *Corresponding author. E-mail: qiujn@dlut.edu.cn*

ABSTRACT This study investigates the performance of four machine learning (ML) algorithms to evaluate the earthquake-induced liquefaction potential of soil based on the cone penetration test field case history records using the Bayesian belief network (BBN) learning software Netica. The BBN structures that were developed by ML algorithms-K2, hill climbing (HC), tree augmented naive (TAN) Bayes, and Tabu search were adopted to perform parameter learning in Netica, thereby fixing the BBN models. The performance measure indexes, namely, overall accuracy (*OA*), precision, recall, *F-measure*, and area under the receiver operating characteristic curve, were used to evaluate the training and testing BBN models' performance and highlight the capability of the K2 and TAN Bayes models over the Tabu search and HC models. The sensitivity analysis results showed that the cone tip resistance and vertical effective stress are the most sensitive factors, whereas the mean grain size is the least sensitive factor in the prediction of seismic soil liquefaction potential. The results of this study can provide theoretical support for researchers in selecting appropriate ML algorithms and improving the predictive performance of seismic soil liquefaction potential models.

KEYWORDS seismic soil liquefaction, Bayesian belief network, cone penetration test, parameter learning, structural learning

1 Introduction

A liquefaction hazard evaluation involves the liquefaction potential, initiation of liquefaction, and effects of liquefaction. The former one, i.e., liquefaction potential evaluation, is a prerequisite to the other two and is the major concern of geotechnical engineers. In the past several decades, different methods, pioneered by Seed and Idriss [1], were developed for the evaluation of soil liquefaction potential. Such methods can generally be divided into six groups [2]: field methods; analytical methods; laboratory methods; geographic information system methods; numerical methods; and statistical, soft computing (SC)- and artificial intelligence (AI)-based methods. Several researchers have applied SC- and AI-based techniques in engineering, physics, and mathematical problems and have achieved comparatively satisfactory results [3–5]. Applications of SC- and AI-based techniques, for example, artificial neural network (ANN), support vector machine (SVM), and adaptive neuro fuzzy inference system (ANFIS), have achieved accurate results in engineering, particularly in assessing seismic soil liquefaction potential. Goh [6,7] applied ANN to evaluate soil liquefaction potential using the cone penetration test (CPT) and standard penetration test (SPT) case history records. Pal [8] used the SVM-based classifier to assess soil liquefaction potential using CPT and SPT test data. Xue and Yang [9] employed the ANFIS for the evaluation of seismic soil liquefaction potential using CPT data. Kohestani et al. [10] employed a random forest algorithm to evaluate the soil liquefaction potential from CPT case history records. Hu et al. [11] employed a hybrid approach combining machine learning (ML) algorithms, i.e., K2 and domain knowledge (DK),

Article history: Received May 27, 2019; Accepted Sep 16, 2019

and built a Bayesian belief network (BBN) for seismic soil liquefaction potential assessment using SPT case historic records. Kaveh et al. [12] used the patient ruled induction method (PRIM) to assess the occurrence and non-occurrence of soil liquefaction. Hoang and Bui [13] developed a model based on a hybridization of the kernel fisher discriminate analysis and least squares SVM for evaluating the earthquake-induced liquefaction potential. More recently, Zhou et al. [14] employed the stochastic gradient boosting (SGB) approach for assessing soil liquefaction potential using CPT and SPT data. The above-mentioned methods have attained comparatively promising results. However, the major limitations of most SC- and AI-based techniques, such as the ANN approach, are their black-box nature similar to that of SGB's algorithm, overfitting problems, slow convergence speed, and arrival at local minima [15,16]. The ANFIS model takes too long to build membership functions, whereas the rule base and SVM cannot easily determine insensitive and penalty weight parameters [14]. By contrast, using ML techniques (with or without DK) to build a BBN model from field case history records furnishes several specific advantages compared to other SC- and AI-based methods, which can present understandable semantic interpretations, a suitable framework to tackle cause–effect relations, uncertainty analysis, and probability reasoning. Thus, seismic soil liquefaction potential evaluation poses substantial challenges and major concerns in geotechnical engineers. Therefore, a more systematic and in-depth study is necessary in predicting the liquefaction potential induced by earthquakes using ML algorithms.

In in situ tests, the CPT has certain advantages, such as a nearly continuous soil profile along the depth of the explored soil layer, and is more consistent and repeatable than other in situ test methods. Moreover, many researchers have used CPT results for assessing liquefaction potential [17,18]. Particularly, the authors have focused on CPT case history data for the development of BBN models using ML algorithms.

This study has significance in several ways. First, this research asserted different heuristic or general-purpose search algorithms for the development of BBN models for seismic soil liquefaction potential evaluation based on CPT case history records. Second, it presents a sensitivity analysis. Third, data division for training and testing data sets was performed with due attention to statistical aspects, such as the mean, standard deviation, and coefficient of variation (COV) of the data sets. The splitting of the data sets was performed to identify the predictive ability and generalization performance of the developed models and to evaluate them better. Fourth, data discretization was conducted to reduce and elucidate the data set, develop the model quickly and easily, and acquire easily interpretable outputs in this study.

The structure of this paper is as follows: Section 2 reviews the basic principles of the BBN and data set and its preprocessing; Section 3 describes the construction of BBN models and their performance metrics; Section 4 illustrates the major findings and discussion of this study; and Section 5 sets out the most relevant conclusions and future work of the study.

2 Materials and methods

2.1 Basic principles of BBN

BBN is a graphical model that allows a probabilistic relationship between a set of variables [19]. The BBN approach is rooted in the utilization of Bayes' theorem. A BBN is a triplet (V, A, P), where V is a set of variables; A is a set of arcs, which, together with variables (V), represents a directed acyclic graph $G = (V, A)$; and P is a set of conditional probabilities of all the variables given with relevant parents.

Thus, the posterior probability in the BBN may be determined by Bayes' formulas and conditional independence rule in accordance with the following:

$$P(X_i|Y) = \frac{P(Y|X_i) \cdot P(X_i)}{P(Y)}, \tag{1}$$

$$P(Y|X_i) = \frac{P(x_1,...,x_n|Y) \cdot P(Y)}{P(x_1,...,x_n)}, \tag{2}$$

$$P(x_1,..., x_n) = \prod_{i=1}^{n} P(x_i|\pi(x_i)), \tag{3}$$

where $x_1,...,x_n$ and Y are random variables; $P(X_i|Y)$ is the posterior probability of variable X_i given evidence Y; $P(X_i)$ and $P(Y)$ are the prior probabilities of variables X_i and Y; $P(Y|X_i)$ is the likelihood and is proportional to the conditional probability of observing a particular event given evidence X_i; $P(x_1,\ldots,x_n)$ is the joint probability of variables $x_1,...,x_n$; and $\pi(x_i)$ is a set of values for the parents of X_i. Equation (1) presents backward inferring, and Eq. (2) presents forward reasoning.

In seismic soil liquefaction, the relationship between the historical data of the liquefaction manifestation and its factors may be employed as an effective prior knowledge to determine the structure of a BBN model for seismic liquefaction potential. Hence, prior knowledge was utilized to construct a BBN structure to avoid unreasonable relationships led by overfitting, and parameter learning was made to acquire a conditional probability table for nodes in the structure.

2.1.1 Structure learning

Structure learning is the basic step of BBN learning, and the efficient structure learning is the key to develop the

optimal network structure. Common ML methods are K2, tree augmented naive (TAN) Bayes, Tabu search, and hill climbing (HC) algorithms. To learn the network from the data, different heuristics (K2, HC, and TAN Bayes) or general-purpose (Tabu) ML algorithms are used. A concise overview of these algorithms is given in Table 1. Readers can refer to the corresponding reference materials for more information.

Table 1 Machine learning algorithms for the network structure

machine learning algorithm	description
K2	K2 [20] adds arcs with a fixed topological ordering of variables. In this method, the ordering is primarily set as a naive Bayes network where the target class variable is the first in the ordering.
HC	HC [21] adds and deletes arcs with no fixed ordering of variables. This process is iterated unless the highest value of the measurement score (e.g., local Bayes) is achieved.
Tabu search	Tabu search [22] is an optimal HC algorithm. This algorithm utilizes a Markov Blanket correction to the network structure after learning the network structure.
TAN Bayes	In TAN Bayes [23], the tree is built by computing the maximum-weight spanning tree applying Chow and Liu's algorithm [24].

2.1.2 Parameter learning

Parameter learning is performed to identify the conditional probability distribution for each node under a given BBN model. Maximum likelihood estimation, expectation maximization, and gradient descent are the three main algorithms for acquiring the conditional probability table. The maximum likelihood estimation is the swiftest and easiest, based entirely on data and independent of prior probabilities, so it does not apply to models containing hidden variables, and the data set includes several missing values [25]. Expectation maximization and gradient descent algorithms work through an iterative process; however, expectation maximization is appropriate for data that contain missing values. In short, expectation maximization learning repeatedly uses BBNs and uses them to perform a desired expectation (E) step and then maximize (M) step to find a better network [26].

2.2 Data set and discretization of parameters

The CPT-based soil liquefaction data set from previous earthquakes were considered and applied to investigate the four ML algorithms (K2, HC, TAN Bayes, and Tabu search, see Table 1). Stark and Olson [27] collected a database of published research articles, which consists of 180 liquefaction and non-liquefaction case history records gathered from the field performance observations of nine different earthquakes around the world from 1964 to 1989, such as the Niigata earthquake in 1964, San Fernando Valley earthquake in 1971, Haicheng earthquake in 1975, Tangshan earthquake in 1976, Vrancea earthquake in 1977, Imperial Valley earthquake in 1979, Nihonkai-Cho earthquake 1983, Sanguenay earthquake in 1988, and Loma Prieta earthquake in 1989. After eliminating 10 case records owing to missing values, 170 completed case history data were preserved. The numbers of non-liquefied and liquefied case history records are 66 and 104 in the CPT database, respectively. The six input parameters utilized for the liquefaction potential evaluation are the earthquake magnitude (M), peak ground acceleration a_{max} (g), cone tip resistance (q_c, MPa), mean grain size (D_{50}), vertical effective stress (σ'_v, kPa), and total vertical stress (σ_v, kPa). Readers can refer to the study by Stark and Olson [27] for further information regarding these case history records. The statistical characteristics of the mean, standard deviation, and COV of the data set utilized in this study are shown in Table 2.

BBN has a strong capability to deal with discrete variables but is poor in processing continuous variables, so the six significant factors of seismic soil liquefaction potential should be converted into discrete values before developing the BBN ML models as per the possible factor range and expert knowledge, as shown in Table 3. Previous studies (Tranfield et al. [28]; Okoli and Schabram [29]; Zhang [30]; Hu et al. [31]; Ahmad et al. [32–34]) contributed detailed understanding to lead the selection of variables, discretization, and classification in the present study. The optimal multisplitting discretization algorithm [35] can be used to determine the optimal subdivisions to discretize factors for BBNs in case one has limited knowledge or experts cannot furnish accurate classification recommendations.

Table 2 Statistical aspects of the data set

factor	minimum	maximum	mean	standard deviation	coefficient of variation
earthquake magnitude, M	5.90	7.80	7.30	0.61	0.08
peak ground acceleration, a_{max} (g)	0.10	0.60	0.28	0.13	0.47
cone tip resistance, q_c (MPa)	0.38	26.00	6.41	5.24	0.82
mean grain size, D_{50} (mm)	0.016	0.48	0.17	0.10	0.61
vertical effective stress, σ'_v (kPa)	13.90	227.50	78.59	44.86	0.57
total vertical stress, σ_v (kPa)	16.70	296.30	114.43	66.25	0.58

Table 3 Grading standards for seismic soil liquefaction factors

factors of seismic soil liquefaction	number of grade	explanation	range
earthquake magnitude, M	4	super	$8 \leqslant M$
		big	$7 \leqslant M < 8$
		strong	$6 \leqslant M < 7$
		medium	$4.5 \leqslant M < 6$
peak ground acceleration, a_{max} (g)	4	super	$0.40 \leqslant a_{max}$
		high	$0.30 \leqslant a_{max} < 0.40$
		medium	$0.15 \leqslant a_{max} < 0.30$
		low	$0 \leqslant a_{max} < 0.15$
cone penetration resistance, q_c (MPa)	4	super	$10 \leqslant q_c$
		big	$7 \leqslant q_c < 10$
		medium	$3.5 \leqslant q_c < 7$
		small	$0 \leqslant q_c < 3.5$
mean grain size, D_{50} (mm)	4	super	$2 \leqslant D_{50}$
		big	$0.425 \leqslant D_{50} < 2$
		medium	$0.075 \leqslant D_{50} < 0.425$
		small	$0 < D_{50} < 0.075$
vertical effective stress, σ'_v (kPa)	4	super	$150 \leqslant \sigma'_v$
		big	$100 \leqslant \sigma'_v < 150$
		medium	$50 \leqslant \sigma'_v < 100$
		small	$0 \leqslant \sigma'_v < 50$
total vertical stress, σ_v (kPa)	4	super	$165 \leqslant \sigma_v$
		big	$110 \leqslant \sigma_v < 165$
		medium	$55 \leqslant \sigma_v < 110$
		small	$0 \leqslant \sigma_v < 55$
liquefaction potential	2	no	0
		yes	1

3 Development of models and performance metric

3.1 BBN models

To develop the models, the data set was divided into training and testing data sets, and the details are summarized in Tables 4 and 5, respectively.

A training data set is needed to train the models. Authors used 70% of the data, i.e., 119 out of 170 case histories are taken into account for the training set.

A testing data set is needed to predict the developed model performance. In this study, the remaining 30% of the data, i.e., 51 out of the 170 case histories, were utilized as the testing data set.

The statistical parameters of the input variables include the minimum, maximum, mean, standard deviation, and COV of the training and testing data sets, which are shown in Table 6. The data set splitting was performed to determine the generalization performance and predictive ability of the developed models. The similar performance of the training and testing data sets demonstrates that the developed models may be applied for the trained ranges. As indicated in Table 6, the ranges of the input and output parameters in the testing also exist in the training data sets. The statistical consistency of the training and testing data sets optimizes the BBN models' performance and subsequently assists in evaluating them better.

The development of a BBN model primarily consists of the following steps.

1) Structure learning: identify the factor variables, i.e., nodes associated with the study object, and then find dependencies or independent relationships among the nodes to develop a directed acyclic network structure.

2) Parameter learning: according to the given BBN structure, the conditional probability table of each node of the BBN model is learned using data.

The development of the BBN structure comprises of the following methods: 1) The BBN structure based on experts' knowledge is referred as DK; 2) ML algorithms are used to learn from the data; 3) DK and ML algorithms are combined using data fusion methodology to derive the BBN structure. In this study, the BBN structures suggested by Tesfamarian and Liu [36] were adopted using ML algorithms to learn from the data (see Fig. 1). The selected ML algorithms were driven by different principles and metrics, such as the K2 algorithm, which is based on the search-and-score paradigm; HC algorithm adds and deletes arcs with no established ordering of variables; Tabu search algorithm performs HC unless reaching a local optimal; and in TAN Bayes algorithm, the tree is created by computing the maximum weight spanning tree by utilizing Chow and Liu's algorithm [24]. The network structures shown in Fig. 1 are comprised of seven nodes and multiple lines. The seven nodes relate to seven variables, and lines connecting these nodes point out associations between

Table 4 Summary of training data

earthquake	D_{50} (mm)	σ'_v (kPa)	σ_v (kPa)	a_{max} (g)	M	q_c (MPa)	liquefaction
1964 Niigata	0.33	35.3	52	0.16	7.5	3.14	yes
	0.33	51	85.3	0.16	7.5	1.57	yes
	0.33	81.4	149.1	0.16	7.5	5.49	yes
	0.33	61.8	89.2	0.16	7.5	5.34	yes
	0.33	78.5	124.5	0.16	7.5	7.8	yes
	0.33	117.1	206.9	0.16	7.5	9.51	yes
	0.3	45.1	84.3	0.16	7.5	7.85	no
	0.3	49	93.2	0.16	7.5	14.27	no
1971 San Fernando Valley	0.058	166.1	167.6	0.5	6.4	6.37	yes
	0.073	182.6	200.5	0.5	6.4	6.86	yes
	0.052	119.7	125.7	0.5	6.4	3.14	yes
	0.045	138.9	164	0.5	6.4	0.69	yes
	0.16	161.7	209.5	0.5	6.4	9.81	no
	0.053	170.7	227.4	0.5	6.4	8.73	no
	0.072	202.1	290.3	0.5	6.4	9.32	no
	0.042	86.8	89.8	0.5	6.4	0.69	yes
	0.095	146.7	209.5	0.5	6.4	10.79	no
	0.069	152.7	221.4	0.5	6.4	13.73	no
	0.082	190.2	296.3	0.5	6.4	6.86	no
	0.072	95.8	98.8	0.5	6.4	1.96	yes
	0.055	103.3	113.7	0.5	6.4	0.69	yes
	0.067	146.7	200.5	0.5	6.4	0.69	no
	0.13	166.2	239.4	0.5	6.4	4.9	no
	0.062	175.2	257.4	0.5	6.4	9.81	no
	0.045	190.2	287.3	0.5	6.4	15.69	no
	0.051	119.7	122.7	0.5	6.4	1.96	yes
	0.1	130.2	143.6	0.5	6.4	1.96	yes
1975 Haicheng	0.07	50	74.6	0.15	7.3	0.65	yes
	0.08	41.2	55.9	0.15	7.3	0.53	yes
	0.02	76.5	130.5	0.15	7.3	0.38	yes
	0.016	45.6	65.2	0.15	7.3	1.3	yes
	0.016	105.2	191	0.15	7.3	0.73	no
1976 Tangshan	0.25	83.4	145.1	0.4	7.8	5.59	yes
	0.3	90.2	158.9	0.4	7.8	7.45	yes
	0.17	16.7	16.7	0.4	7.8	1.47	yes
	0.17	20.6	24.5	0.4	7.8	0.98	yes
	0.17	24.5	33.3	0.4	7.8	4.9	yes
	0.14	33.3	37.3	0.4	7.8	2.45	yes
	0.14	42.2	55.9	0.4	7.8	2.55	yes
	0.16	51	74.5	0.4	7.8	3.14	yes
	0.16	56.9	87.3	0.4	7.8	5.69	yes
	0.16	100	177.5	0.4	7.8	8.24	yes
	0.12	34.3	50	0.4	7.8	4.02	yes
	0.17	26.5	28.4	0.4	7.8	5.39	yes

(*Continued*)

earthquake	D_{50} (mm)	σ'_v (kPa)	σ_v (kPa)	a_{max} (g)	M	q_c (MPa)	liquefaction
	0.32	39.2	55.9	0.4	7.8	8.83	yes
	0.48	20.6	22.6	0.4	7.8	6.86	yes
	0.48	25.5	33.3	0.4	7.8	1.16	yes
	0.48	32.4	47.1	0.4	7.8	4.16	yes
	0.2	108.9	156.9	0.4	7.8	15.46	no
	0.14	73.5	97.1	0.2	7.8	17.42	no
	0.17	76.5	87.3	0.2	7.8	1.62	yes
	0.17	81.4	97.1	0.2	7.8	3.58	yes
	0.31	36.3	53.9	0.2	7.8	4.9	yes
	0.18	46.1	74.5	0.2	7.8	2.85	yes
	0.18	59.8	103	0.2	7.8	5.94	yes
	0.17	21.6	22.6	0.2	7.8	12.98	no
	0.17	25.5	31.4	0.2	7.8	12.81	no
	0.17	29.4	39.2	0.2	7.8	16.27	no
	0.26	57.9	57.9	0.2	7.8	10.39	no
	0.26	65.7	74.5	0.2	7.8	11.07	no
	0.16	43.1	74.5	0.2	7.8	4.9	yes
	0.14	46.1	68.6	0.2	7.8	2.2	yes
	0.14	48.1	72.6	0.2	7.8	2.6	yes
	0.16	34.3	52	0.2	7.8	4.31	yes
	0.16	38.2	59.8	0.2	7.8	2.94	yes
	0.08	79.4	153	0.2	7.8	8.83	yes
	0.07	51	93.2	0.2	7.8	1.08	yes
	0.08	103.9	205	0.1	7.8	15.2	no
	0.08	107.9	212.8	0.1	7.8	6.37	no
	0.1	52	89.2	0.1	7.8	8.83	no
	0.28	100	158.9	0.1	7.8	18.57	no
	0.16	43.1	43.1	0.2	7.8	3.45	yes
	0.16	50	57.9	0.2	7.8	2.68	yes
	0.21	51	59.8	0.2	7.8	4.04	yes
	0.32	66.7	93.2	0.2	7.8	5.74	yes
	0.13	47.1	48.1	0.2	7.8	1.84	yes
	0.22	75.5	111.8	0.2	7.8	7.85	no
	0.067	110.6	223.6	0.2	7.8	4.46	no
	0.067	120.4	244.2	0.2	7.8	5.68	no
	0.062	54.3	111.8	0.2	7.8	2.43	yes
	0.062	55.3	118.7	0.2	7.8	1.54	yes
	0.067	104.6	215.7	0.2	7.8	2.11	yes
	0.067	109.7	225.5	0.2	7.8	2.55	yes
	0.067	101.8	208.9	0.2	7.8	2.68	yes
	0.067	104.6	214.8	0.2	7.8	1.75	yes
	0.067	106.5	206.9	0.2	7.8	7.49	no
1977 Vrancea	0.2	47.1	78.5	0.22	7.2	5.12	yes
	0.2	53.9	93.2	0.22	7.2	3.66	yes

(*Continued*)

earthquake	D_{50} (mm)	σ'_v (kPa)	σ_v (kPa)	a_{max} (g)	M	q_c (MPa)	liquefaction
	0.2	62.8	111.8	0.22	7.2	3.05	yes
	0.2	71.6	130.4	0.22	7.2	1.29	yes
	0.2	80.4	149.1	0.22	7.2	5.12	yes
1979 Imperial Valley	0.11	44.5	62.8	0.6	6.6	19.9	no
	0.11	44.5	62.8	0.6	6.6	1.8	yes
	0.07	13.9	31.4	0.2	6.6	2	yes
	0.15	31.6	78.5	0.2	6.6	4.9	yes
1983 Nihonkai Cho	0.32	47.1	56.9	0.23	7.7	9.81	no
	0.32	53	71.6	0.23	7.7	15.69	no
	0.32	63.7	94.1	0.23	7.7	15.08	no
	0.32	51	62.8	0.23	7.7	4.02	yes
	0.32	65.7	94.1	0.23	7.7	7.8	yes
	0.32	73.5	111.8	0.23	7.7	8.8	yes
1988 Sanguenay	0.1	43.1	50.8	0.25	5.9	4.26	no
	0.1	53.1	70.4	0.25	5.9	4.91	no
	0.1	63	90	0.25	5.9	2.76	yes
	0.1	72.8	109.6	0.25	5.9	5.71	no
	0.1	92.4	148.9	0.25	5.9	7.77	no
1989 Loma Prieta	0.253	88.5	118.4	0.24	7.1	19	no
	0.275	67.2	77.6	0.24	7.1	13.94	no
	0.361	78.9	100	0.24	7.1	18	no
	0.35	100.1	140.9	0.24	7.1	13	no
	0.16	83.6	115	0.24	7.1	0.75	yes
	0.07	66.2	108.9	0.16	7.1	1.9	yes
	0.27	87.1	128.8	0.29	7.1	4.7	yes
	0.26	100.6	154.5	0.29	7.1	10	yes
	0.3	82.4	111.8	0.29	7.1	8.7	yes
	0.3	84.6	116.5	0.29	7.1	6.5	yes
	0.22	50.5	65.2	0.27	7.1	5.3	yes
	0.22	50.5	65.2	0.3	7.1	6.1	yes
	0.22	54.9	74.6	0.3	7.1	26	no

variables. Figure 1 clearly shows that K2 has all input parameters at the same level, and the HC search algorithm determines the relationship between M and a_{max}. The TAN Bayes and Tabu search ML algorithms presented counter-intuitive results with regard to parameter dependence. For instance, both algorithms indicate that M depends on D_{50}. Various ML algorithms when performed on the same set of attributes and their instances present fairly discriminated structures. The chosen ML algorithms are driven by different principles and metrics, so the resulting models differ somewhat in the edges they extract.

The network structures are created in Netica free version software distributed by Norsys Software Corporation under the Norsys License Agreement to perform parameter learning to acquire the conditional probability distribution of the nodes. BBN models are determined to assess seismic soil liquefaction potential, as shown in Fig. 2.

3.2 Performance metrics

The BBN models that were established by ML algorithms in the Netica environment were numerically evaluated and compared using scalar performance measures. These metrics may be calculated from Table 7.

In a binary class case, i.e., liquefaction and non-liquefaction, a single prediction has four possible outcomes. The true negative (*TN*) and true positive (*TP*) are correct classifications [37]. A false positive (*FP*) takes

Table 5 Summary of testing data

earthquake	D_{50} (mm)	σ'_v (kPa)	σ_v (kPa)	a_{max} (g)	M	q_c (MPa)	liquefaction
1964 Niigata	0.33	56.9	97.1	0.16	7.5	7.06	yes
1971 San Fernando Valley	0.4	212.5	260.3	0.5	6.4	11.77	no
	0.068	218.5	272.3	0.5	6.4	19.32	no
	0.044	227.5	290.3	0.5	6.4	21.57	no
	0.07	154.2	194.5	0.5	6.4	1.77	no
	0.057	182.7	251.4	0.5	6.4	5.39	no
	0.05	131.7	179.6	0.5	6.4	7.06	no
	0.06	178.2	272.3	0.5	6.4	8.83	no
	0.038	110.8	128.7	0.5	6.4	2.94	yes
	0.059	155.7	218.5	0.5	6.4	1.96	no
	0.24	154.2	191.5	0.5	6.4	20.6	no
1975 Haicheng	0.035	80.9	139.8	0.15	7.3	1.2	yes
1976 Tangshan	0.06	41.2	55.9	0.4	7.8	1.67	yes
	0.25	67.7	111.8	0.4	7.8	9.22	yes
	0.16	72.6	119.6	0.4	7.8	3.43	yes
	0.12	28.4	37.3	0.4	7.8	1.67	yes
	0.12	28.4	39.2	0.4	7.8	3.43	yes
	0.16	69.6	74.5	0.4	7.8	11.25	no
	0.21	54.9	57.9	0.2	7.8	11.17	no
	0.21	63.7	76.5	0.2	7.8	11.89	no
	0.19	24.5	28.4	0.2	7.8	1.01	yes
	0.26	59.8	61.8	0.2	7.8	8.94	no
	0.16	40.2	68.6	0.2	7.8	1.9	yes
	0.14	53.9	97.1	0.1	7.8	1.96	yes
	0.1	56.9	99	0.1	7.8	2.45	no
	0.1	61.8	109.8	0.1	7.8	16.18	no
	0.25	66.7	89.2	0.1	7.8	13.39	no
	0.25	77.5	111.8	0.1	7.8	13.85	no
	0.21	49	55.9	0.2	7.8	3.23	yes
	0.21	55.9	70.6	0.2	7.8	2.88	yes
	0.15	51	59.8	0.2	7.8	2.94	yes
	0.32	77.6	103.9	0.2	7.8	8.83	yes
	0.17	62.8	72.6	0.2	7.8	2.5	yes
	0.17	63.7	74.5	0.2	7.8	4.41	yes
	0.17	77.5	103.9	0.2	7.8	4.16	yes
	0.062	57.2	111.8	0.2	7.8	8.31	no
	0.067	101.8	208.9	0.2	7.8	1.42	yes
1979 Imperial Valley	0.08	44.5	62.8	0.6	6.6	7	no
1983 Nihonkai Cho	0.32	45.1	53	0.23	7.7	1.76	yes
1988 Sanguenay	0.1	82.6	129.3	0.25	5.9	6.51	no
	0.1	102.2	168.5	0.25	5.9	7.77	no
1989 Loma Prieta	0.303	84	118.4	0.24	7.1	16.75	no
	0.239	63	69.4	0.24	7.1	9.75	no
	0.178	59.1	64.1	0.24	7.1	3.35	yes

(*Continued*)

earthquake	D_{50} (mm)	σ'_v (kPa)	σ_v (kPa)	a_{max} (g)	M	q_c (MPa)	liquefaction
	0.197	81.8	120.6	0.24	7.1	1.2	yes
	0.244	117.1	131.9	0.24	7.1	5.5	no
	0.1	36.4	45.6	0.14	7.1	1.3	yes
	0.1	39.5	44.1	0.14	7.1	1.5	yes
	0.12	51.8	60.4	0.14	7.1	2.5	no
	0.07	66.2	108.9	0.16	7.1	1.7	yes
	0.07	66.2	108.9	0.16	7.1	1.5	yes

Table 6 Ranges of seismic soil liquefaction factors for training and testing data sets

seismic soil liquefaction factor	data set	minimum	maximum	mean	standard deviation	coefficient of variation
earthquake magnitude, M	training	5.9	7.8	7.31	0.60	0.08
	testing	5.9	7.8	7.27	0.62	0.09
peak ground acceleration, a_{max} (g)	training	0.1	0.6	0.29	0.13	0.45
	testing	0.1	0.6	0.28	0.15	0.52
cone penetration resistance, q_c (MPa)	training	0.38	26	6.39	5.13	0.80
	testing	1.01	21.57	6.46	5.54	0.86
mean grain size, D_{50} (mm)	training	0.016	0.48	0.17	0.11	0.62
	testing	0.035	0.4	0.16	0.09	0.58
vertical effective stress, σ'_v (kPa)	training	13.9	202.1	76.40	42.25	0.55
	testing	24.5	227.5	83.68	50.50	0.60
total vertical stress, σ_v (kPa)	training	16.7	296.3	114.04	65.71	0.58
	testing	28.4	290.3	115.34	68.13	0.59

place when the outcome is wrongly classified as positive, and a false negative (*FN*) takes place when the output is wrongly predicted as negative. The overall accuracy (*OA*) is the percentage of correctly classified cases in all of the data. The value of *OA* is calculated as follows:

$$OA = \frac{TP + TN}{TP + FN + FP + TN}. \tag{4}$$

In the seismic soil liquefaction problem, liquefaction cases are usually more than the non-liquefaction cases, so evaluating the predictive ability based on the *OA* alone may be deceptive owing to the class imbalance in the data set because it becomes higher when the liquefied samples in the majority class are favorably predicted. Therefore, the predictive capability evaluation based on the *OA* alone may be misleading. Thus, the best choice is *F-measure*, which is the harmonic mean of recall and precision employing equal weights for both. Precision refers to the accuracy of predictions for a positive or negative class, and recall measures the accuracy of predictions considering only predicted values. They can be found in the confusion matrix as

$$Precision = \frac{TP}{TP + FP} \text{ or } \frac{TN}{FN + TN}, \tag{5}$$

$$Recall = \frac{TP}{TP + FN} \text{ or } \frac{TN}{FP + TN}, \tag{6}$$

$$F\text{-}measure = \frac{2 \times Precision \times Recall}{Precision + Recall}. \tag{7}$$

The *F-measure* ranges from 0 (worst value) to 1 (best value).

The area under the receiver operating characteristic (ROC) curve (AUC) is the area between the horizontal axis and ROC curve that gives a comprehensive scalar value on the expected performance of the model. The AUC was employed to summarize the ROC curve. The ROC curve gives five degrees of rating [38]: excellent (0.9–1), good (0.8–0.9), fair (0.7–0.8), poor (0.6–0.7), and not discriminating (0.5–0.6).

Concisely, a model with a good *OA*, large AUC, and high F-measure concurrently depicts an ideal model as class imbalance, and the sampling bias is not simply eluded

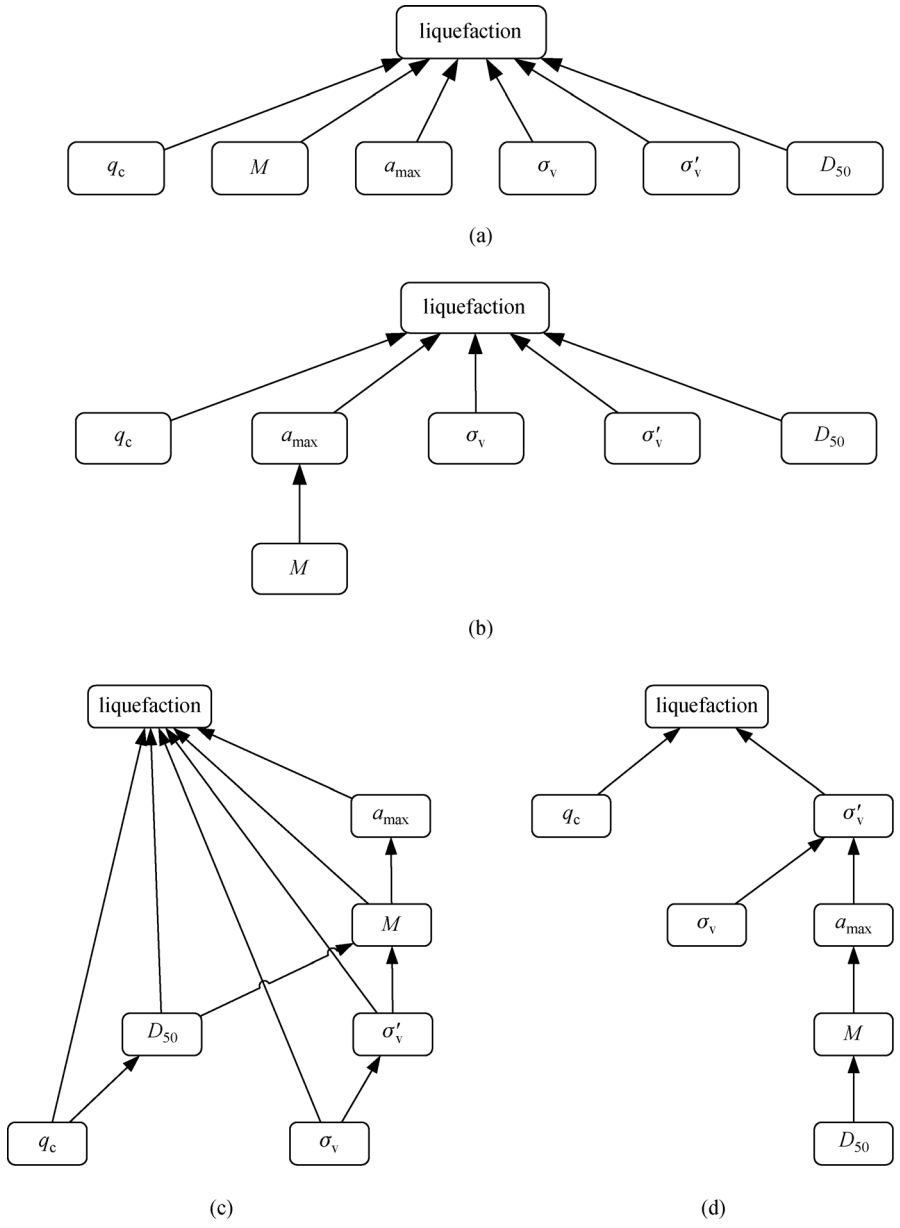

Fig. 1 Bayesian belief network through different machine learning algorithms. (a) K2; (b) HC; (c) TAN Bayes; (d) Tabu search.

in the soil liquefaction study. Thus, evaluating the performance of the soil liquefaction potential model using a single metric alone will be misleading. Therefore, the metrics of *OA*, AUC, recall, precision, and *F-measure* for liquefaction and non-liquefaction instances should be comprehensively analyzed.

4 Results and discussions

4.1 Performance comparison of the training and testing data sets

The performance comparison of the BBN models was conducted for the training and testing data sets. The ratio of the number of liquefied case history records to non-liquefied case history records is 1.90:1 for the training data set. Clearly, there is a class imbalance problem in the training data set. The ratios for the testing and total data sets are 1.04:1 and 1.58:1, respectively. Seismic soil liquefaction history data usually exhibit class imbalances, in which one event, i.e., liquefaction, is delineated by a large number of events, whereas the non-liquefaction event is presented by scarcely any [39]. Moreover, the data exhibit a sampling bias, and the sample distribution category differs from the actual distribution category in the population [39]. Evidently, no explicit agreement has come out on whether a data set should have the same

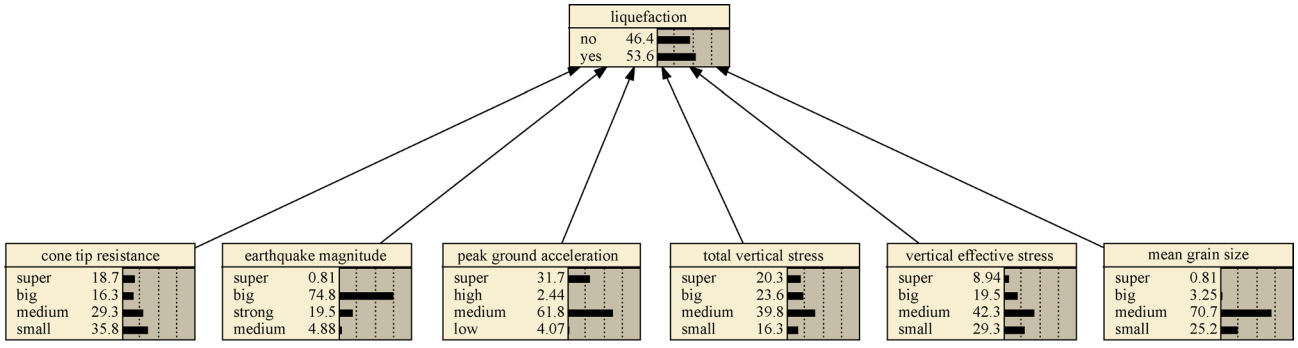
liquefaction
no 46.4
yes 53.6
cone tip resistance
super 18.7
big 16.3
medium 29.3
small 35.8
earthquake magnitude
super 0.81
big 74.8
strong 19.5
medium 4.88
peak ground acceleration
super 31.7
high 2.44
medium 61.8
low 4.07
total vertical stress
super 20.3
big 23.6
medium 39.8
small 16.3
vertical effective stress
super 8.94
big 19.5
medium 42.3
small 29.3
mean grain size
super 0.81
big 3.25
medium 70.7
small 25.2

(a)

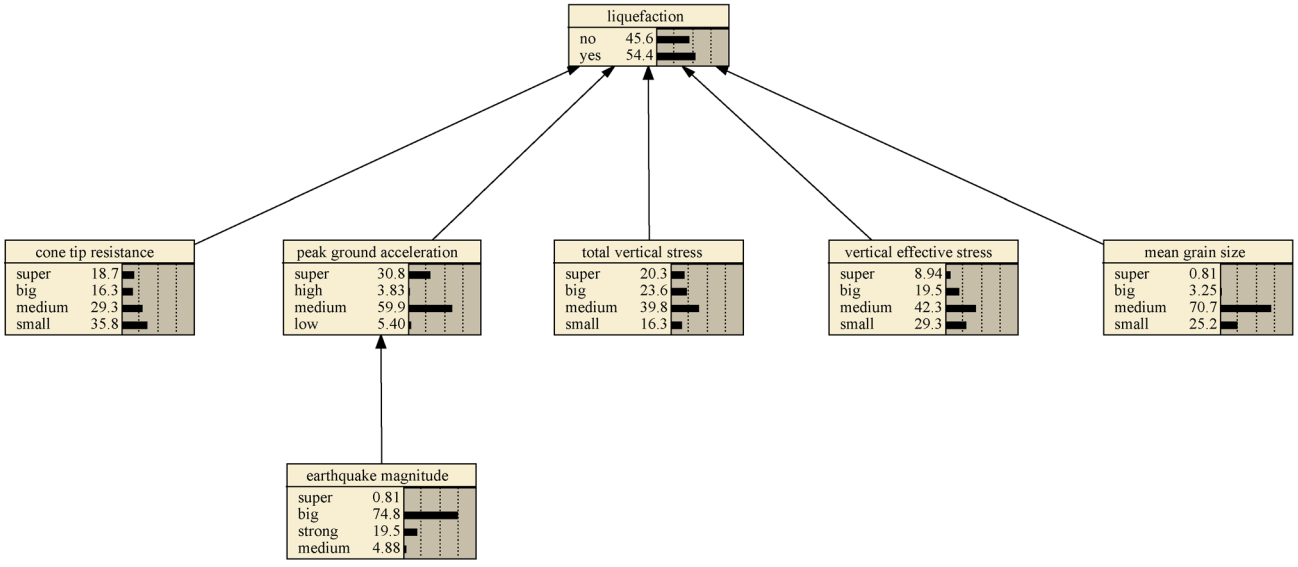
liquefaction
no 45.6
yes 54.4
cone tip resistance
super 18.7
big 16.3
medium 29.3
small 35.8
peak ground acceleration
super 30.8
high 3.83
medium 59.9
low 5.40
total vertical stress
super 20.3
big 23.6
medium 39.8
small 16.3
vertical effective stress
super 8.94
big 19.5
medium 42.3
small 29.3
mean grain size
super 0.81
big 3.25
medium 70.7
small 25.2
earthquake magnitude
super 0.81
big 74.8
strong 19.5
medium 4.88

(b)

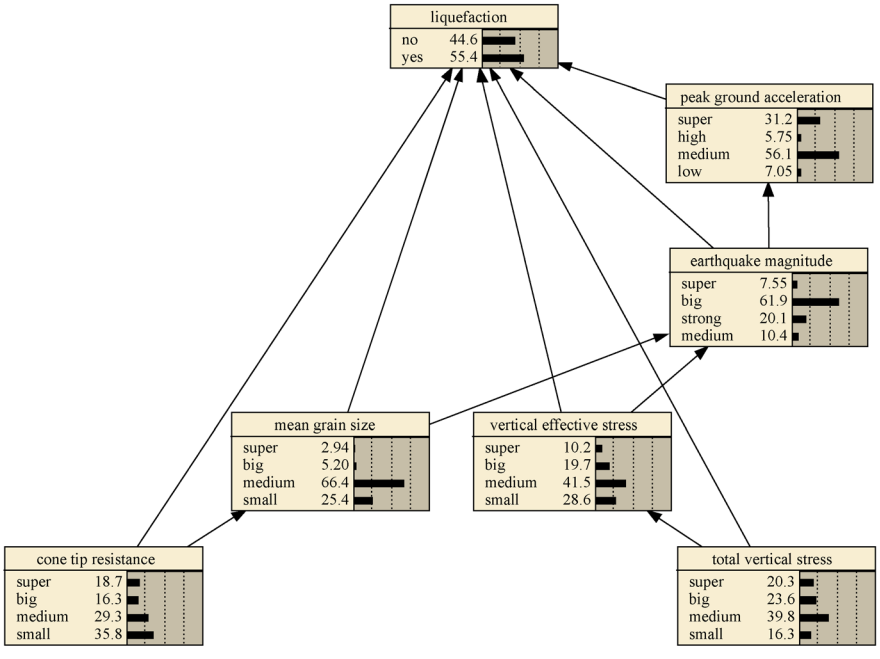
liquefaction
no 44.6
yes 55.4
peak ground acceleration
super 31.2
high 5.75
medium 56.1
low 7.05
earthquake magnitude
super 7.55
big 61.9
strong 20.1
medium 10.4
mean grain size
super 2.94
big 5.20
medium 66.4
small 25.4
vertical effective stress
super 10.2
big 19.7
medium 41.5
small 28.6
cone tip resistance
super 18.7
big 16.3
medium 29.3
small 35.8
total vertical stress
super 20.3
big 23.6
medium 39.8
small 16.3

(c)

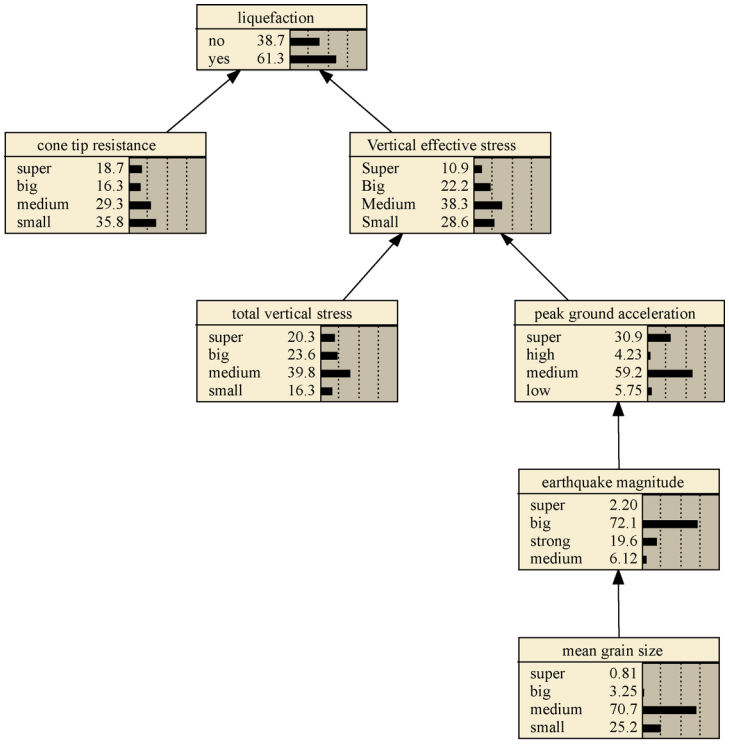

(d)

Fig. 2 BBN machine learning models after parameter learning in Netica 6.02. (a) K2; (b) HC; (c) TAN Bayes; (d) Tabu search.

Table 7 Typical confusion matrix

item		predicted class		gross
		yes	no	
actual class	yes	true positive (*TP*)	false negative (*FN*)	actual positive, $AP = TP + FN$
	no	false positive (*FP*)	true negative (*TN*)	actual negative, $AN = FP + TN$
gross		predicted positive, $PP = TP + FP$	predicted negative, $PN = FN + TN$	$TP + FN + FP + TN$

number of classes or a special class distribution (optimal imbalance) to determine the best classifier performance. However, whether the class imbalance depends on the specific situation and, if so, how the priori determines the best imbalance for each situation are not evident. In the literature, most of the discussion focuses on class imbalance, and there is no clear discussion on how the sampling bias and class imbalance interact [39]. Therefore, the *OA* metric cannot be used alone to determine the developed models' performances. As a result, the precision, recall, *F-measure*, and AUC metrics are employed to assess the performances of the BBN ML models. The overall procedure flowchart of the ML algorithms for the seismic soil liquefaction potential evaluation in Netica environment is presented in Fig. 3.

The comparison results of the four models using the training and testing data sets are presented in Table 8. As regards the *OA*, the K2, TAN Bayes, and Tabu search successfully identified the liquefaction and non-liquefaction instances in the testing data set with 84.3137% success rate. The success rate for HC is 78.4314%. Similarly, in the training data set, the *OA* for K2 and TAN Bayes are 97.4790%, and those of BBN HC and Tabu search are 94.1176% and 89.0756%, respectively. K2 and TAN Bayes gave promising results, and the difference in the AUC in the K2 and TAN Bayes is negligible. However, only the *OA* and AUC cannot be employed as indicators to evaluate the performance of the models. Consequently, the liquefaction and non-liquefaction classes were examined individually using the precision, recall, and *F-measure*. In the cases of the liquefaction and non-liquefaction classes, the K2 and TAN Bayes have the highest and at par precision, recall, and *F-measure* values in the training data set, whereas the Tabu search has the highest recall and *F-measure* values for the liquefaction instances in the testing data set. For the non-liquefaction instances in the testing data set, the K2 and TAN Bayes have the highest recall and *F-measure* values. Thus, after inclusive

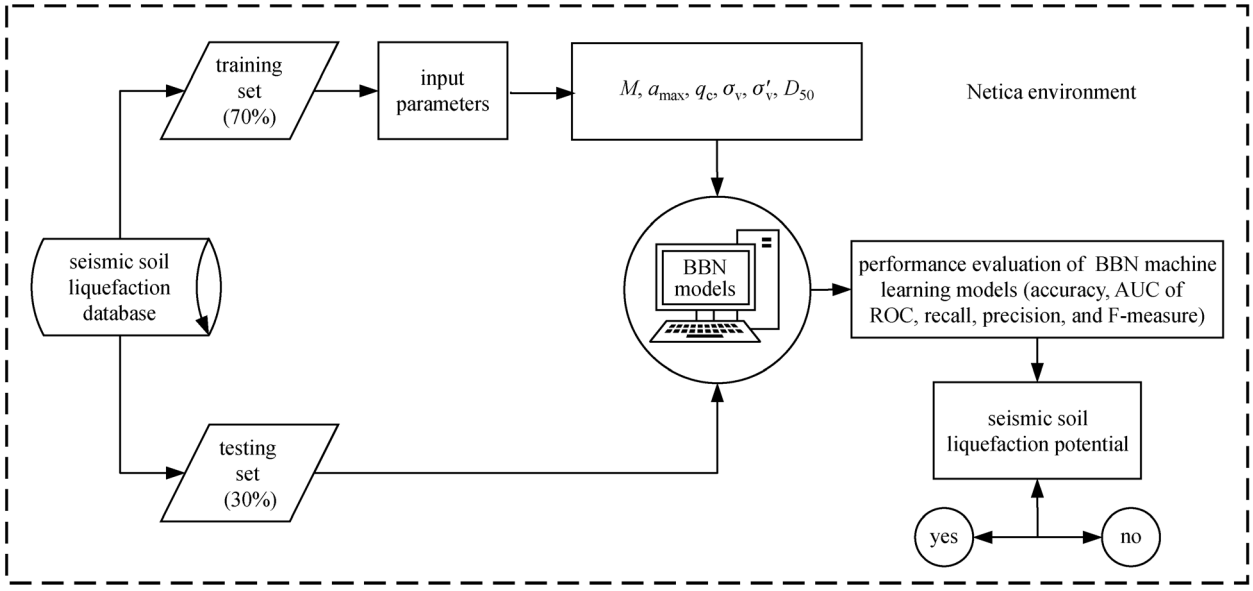

Fig. 3 Overall procedure flowchart for machine learning algorithms for seismic soil liquefaction potential evaluation.

comparisons of the five scalar performance measures, the two BBN models, i.e., K2 and TAN Bayes, present better performance than other BBN ML models, such as HC and Tabu search models. In all, BBN HC showed a relatively worse performance in the training and testing data sets.

4.2 Sensitivity analysis

A very large and diverse literature exists in various domains on sensitivity analysis to determine how each factor affects the uncertainty of the target variable. For instance, Hamdia et al. [40] performed a sensitivity analysis to determine the key input parameters impacting the relation between the tissue structure and mechanics. Ayad et al. [41] performed a sensitivity analysis and showed that soil's parameter variability has a significant effect on soil liquefaction probability. Goh [6] highlighted that the cone tip resistance (q_c) is the most influential factor, whereas the mean grain size (D_{50}) is the least sensitive factor among the input factors for the seismic liquefaction potential evaluation. Pirhadi et al. [42] concluded that the normalized cone penetration tip value (q_{c1N}) is an important factor and has maximum effect on seismic soil liquefaction triggering.

Netica can effectively determine the extent to which any node's findings can affect the beliefs of another node, based on the findings that are currently entered. These findings may have mutual information (entropy reduction) or an expected reduction in the actual variance. In this study, a sensitivity analysis was performed on six input factors with variance of beliefs to determine the effect of each factor on the liquefaction probability. Based on the sensitivity analysis, a basic event that has a relatively large contribution to the probability of a resulting event makes it easier to reduce the probability of these basic events by considering effective measurements, thereby reducing the

Table 8 Performance comparison of BBN machine learning models

model	data set	*OA* (%)	AUC	liquefaction			non-liquefaction		
				precision	recall	*F-measure*	precision	recall	*F-measure*
BBN-K2	training	97.4790	0.9836	0.9747	0.9872	0.9809	0.9750	0.9512	0.9630
	testing	84.3137	0.8954	0.8750	0.8077	0.8400	0.8148	0.8800	0.8462
BBN-HC	training	94.1176	0.9653	0.9277	0.9872	0.9565	0.9722	0.8537	0.9091
	testing	78.4314	0.8538	0.7778	0.8077	0.7925	0.7917	0.7600	0.7755
BBN-TAN Bayes	training	97.4790	0.9830	0.9747	0.9872	0.9809	0.9750	0.9512	0.9630
	testing	84.3137	0.9054	0.8750	0.8077	0.8400	0.8148	0.8800	0.8462
BBN-Tabu search	training	89.0756	0.9437	0.8916	0.9487	0.9193	0.8889	0.7805	0.8312
	testing	84.3137	0.9308	0.7647	1.0000	0.8667	1.0000	0.6800	0.8095

probability of a resulting event. The sensitivity analysis function of Netica software is utilized to determine the factors that have a highest influence on seismic soil liquefaction potential. In Netica, the target node liquefaction in each BBN model is selected to make a sensitivity analysis, and the comparison results of for the four BBN models are presented in Table 9. The mutual information between two nodes can present the dependency of the nodes on each other and the closeness of their relationship [43]. Table 9 shows that the mutual information (0.00500, 0.00947, 0.20065, and 0.01888) of the node cone tip resistance (q_c) is the largest in the BBN K2, HC, Tabu search, and TAN Bayes, respectively, which interprets that it has the strongest influence on liquefaction. Moreover, the mean grain size is the least sensitive factor, which has mutual information (0.00055, 0.00009, and 0.00086) in the three BBN models, i.e., K2, Tabu search, and TAN Bayes, respectively, whereas the earthquake magnitude is the least sensitive in the HC model, which has mutual information of 0.00008. However, after selecting the first two sensitive factors of the four BBN models from Table 9, the factors are identified with three or more overlaps in the results. The authors may affirmed that the cone tip resistance and vertical effective stress are the most sensitive factors to seismic soil liquefaction. Similarly, the least sensitive factor is the mean grain size with three overlaps in the results. These results are highly consistent with those in the literature, e.g., Goh [6].

5 Conclusions and future work

The determination of seismic soil liquefaction potential is a complex geotechnical earthquake engineering problem due to soil heterogeneity, uncertainty, and involvement of many relevant factors affecting a liquefaction occurrence. In the present study, four ML algorithms were applied and investigated to evaluate earthquake-induced liquefaction based on the CPT case history records by utilizing the BBN learning software Netica. The proposed BBN ML models were trained and tested using the CPT case history records of 170 liquefaction and non-liquefaction instances. The performance measure indexes, namely, *OA*, precision, recall, *F-measure*, and AUC, were used to evaluate the training and testing BBN models' performance and highlight the capability of the K2 and TAN Bayes models over the Tabu search and HC models. The K2, TAN Bayes, and Tabu search successfully identified the liquefaction and non-liquefaction instances in the testing data set with 84.3137% success rate. The success rate of HC is 78.4314%. Similarly, in the training data set, the *OA* for TAN and K2 are 97.4790%, and those for HC and Tabu search are 94.1176% and 89.0756%, respectively. Thus, K2 and TAN Bayes gave promising results, and the difference in the AUC of K2 and TAN Bayes is negligible, even though the same approach, i.e., same training and testing data sets, was taken into consideration for the analysis of all models. The results of the sensitivity analysis concluded that the cone tip resistance (q_c) and vertical effective stress (σ'_v) are the most sensitive factors, and the mean grain size (D_{50}) is the least sensitive factor in the evaluation of seismic soil liquefaction potential. The results of this work may present theoretical support for researchers in selecting appropriate ML algorithms and improving the predictive performance of seismic soil liquefaction potential models.

In the future, the authors will take into consideration the following points as an extension of this work.

1) Development of a hybrid systematic approach to improve the model performance for assessing seismic soil

Table 9 Sensitivity analysis result comparisons of seismic soil liquefaction

node	BBN-K2			BBN-HC			BBN-Tabu search			BBN-TAN Bayes		
	mutual info	percent	variance of beliefs	mutual info	percent	variance of beliefs	mutual info	percent	variance of beliefs	mutual info	percent	variance of beliefs
liquefaction	0.99623	100.00000	0.24869	0.99430	100.00000	0.24803	0.96275	100.00000	0.23720	0.99151	100.00000	0.24706
cone tip resistance	0.00500	0.50200	0.00173	0.00947	0.95300	0.00326	0.20065	20.80000	0.06240	0.01880	1.90000	0.00645
vertical effective stress	0.00163	0.16400	0.00056	0.00244	0.24500	0.00084	0.04050	4.21000	0.01346	0.00577	0.58200	0.00198
total vertical stress	0.00140	0.14000	0.00048	0.00236	0.23700	0.00081	0.01221	1.27000	0.00408	0.00371	0.37400	0.00128
earthquake magnitude	0.00106	0.10700	0.00037	0.00008	0.00768	0.00003	0.00050	0.05210	0.00017	0.00607	0.61200	0.00208
peak ground acceleration	0.00056	0.05630	0.00019	0.00090	0.09050	0.00031	0.00222	0.23100	0.00073	0.00374	0.37700	0.00128
mean grain size	0.00055	0.05520	0.00019	0.00055	0.05570	0.00019	0.00009	0.00888	0.00003	0.00086	0.08650	0.00030

liquefaction potential using BBNs that integrate optimal ML algorithms and DK that will call a robust BBN model in the authors' future study

2) Adding more significant factors, such as fine content, critical depth interval, groundwater table depth, depth of soil deposit, and soil behavior type index, to expand the robust BBN model for the assessment of seismic soil liquefaction

3) Adding the nodes of the utility and decision operations in the BBN seismic soil liquefaction model that can be eventually used as an important decision-making information in the case of expected utilities of loss

Acknowledgements The work presented in this paper was part of research sponsored by the National Key Research & Development Plan of China (Nos. 2018YFC1505305 and 2016YFE0200100) and the Key Program of the National Natural Science Foundation of China (No. 51639002).

References

1. Seed H B, Idriss I M. Simplified procedure for evaluating soil liquefaction potential. Journal of the Soil Mechanics and Foundations Division, 1971, 97(9): 1249–1273
2. Daftari A. New approach in prediction of soil liquefaction. Dissertation for the Doctoral Degree. Freiberg, New York: Technische Universität Bergakademie Freiberg, 2015
3. Hamdia K M, Ghasemi H, Zhuang X, Alajlan N, Rabczuk T. Computational machine learning representation for the flexoelectricity effect in truncated pyramid structures. Computers, Materials & Continua, 2019, 59(1): 79–87
4. Anitescu C, Atroshchenko E, Alajlan N, Rabczuk T. Artificial neural network methods for the solution of second order boundary value problems. Computers, Materials & Continua, 2019, 59(1): 345–359
5. Guo H, Zhuang X, Rabczuk T. A deep collocation method for the bending analysis of Kirchhoff plate. Computers, Materials & Continua, 2019, 59(2): 433–456
6. Goh A T. Neural-network modeling of CPT seismic liquefaction data. Journal of Geotechnical Engineering, 1996, 122(1): 70–73
7. Goh A T. Seismic liquefaction potential assessed by neural networks. Journal of Geotechnical Engineering, 1994, 120(9): 1467–1480
8. Pal M. Support vector machines-based modelling of seismic liquefaction potential. International Journal for Numerical and Analytical Methods in Geomechanics, 2006, 30(10): 983–996
9. Xue X, Yang X. Application of the adaptive neuro-fuzzy inference system for prediction of soil liquefaction. Natural Hazards, 2013, 67(2): 901–917
10. Kohestani V, Hassanlourad M, Ardakani A. Evaluation of liquefaction potential based on CPT data using random forest. Natural Hazards, 2015, 79(2): 1079–1089
11. Hu J L, Tang X W, Qiu J N. A Bayesian network approach for predicting seismic liquefaction based on interpretive structural modeling. Georisk: Assessment and Management of Risk for Engineered Systems and Geohazards, 2015, 9(3): 200–217
12. Kaveh A, Hamze-Ziabari S, Bakhshpoori T. Patient rule-induction method for liquefaction potential assessment based on CPT data. Bulletin of Engineering Geology and the Environment, 2018, 77(2): 849–865
13. Hoang N D, Bui D T. Predicting earthquake-induced soil liquefaction based on a hybridization of kernel Fisher discriminant analysis and a least squares support vector machine: A multi-dataset study. Bulletin of Engineering Geology and the Environment, 2018, 77(1): 191–204
14. Zhou J, Li E, Wang M, Chen X, Shi X, Jiang L. Feasibility of stochastic gradient boosting approach for evaluating seismic liquefaction potential based on SPT and CPT case histories. Journal of Performance of Constructed Facilities, 2019, 33(3): 04019024
15. Kecman V. Learning and Soft Computing: Support Vector Machines, Neural Networks, and Fuzzy Logic Models. Cambridge, MA: MIT press, 2001
16. Park D, Rilett L R. Forecasting freeway link travel times with a multilayer feedforward neural network. Computer-Aided Civil and Infrastructure Engineering, 1999, 14(5): 357–367
17. Juang C H, Yuan H, Lee D H, Lin P S. Simplified cone penetration test-based method for evaluating liquefaction resistance of soils. Journal of Geotechnical and Geoenvironmental Engineering, 2003, 129(1): 66–80
18. Moss R, Seed R B, Kayen R E, Stewart J P, Der Kiureghian A, Cetin K O. CPT-based probabilistic and deterministic assessment of in situ seismic soil liquefaction potential. Journal of Geotechnical and Geoenvironmental Engineering, 2006, 132(8): 1032–1051
19. Pearl J. Probabilistic reasoning in intelligent systems: Representation & reasoning. San Mateo, CA: Morgan Kaufmann Publishers, 1988
20. Cooper G F, Herskovits E. A Bayesian method for the induction of probabilistic networks from data. Machine Learning, 1992, 9(4): 309–347
21. Buntine W. A guide to the literature on learning probabilistic networks from data. IEEE Transactions on Knowledge and Data Engineering, 1996, 8(2): 195–210
22. Bouckaert R R. Bayesian belief networks: From construction to inference. Dissertation for the Doctoral Degree. Utrecht: Utrecht University, 1995
23. Friedman N, Geiger D, Goldszmidt M. Bayesian network classifiers. Machine Learning, 1997, 29(2–3): 131–163
24. Chow C, Liu C. Approximating discrete probability distributions with dependence trees. IEEE Transactions on Information Theory, 1968, 14(3): 462–467
25. Spiegelhalter D J, Lauritzen S L. Sequential updating of conditional probabilities on directed graphical structures. Networks, 1990, 20(5): 579–605
26. Lauritzen S L. The EM algorithm for graphical association models with missing data. Computational Statistics & Data Analysis, 1995, 19(2): 191–201
27. Stark T D, Olson S M. Liquefaction resistance using CPT and field case histories. Journal of Geotechnical Engineering, 1995, 121(12): 856–869
28. Tranfield D, Denyer D, Smart P. Towards a methodology for developing evidence-informed management knowledge by means of systematic review. British Journal of Management, 2003, 14(3):

207–222

29. Okoli C, Schabram K. A guide to conducting a systematic literature review of information systems research. Sprouts: Working Papers on Information Systems, 2010, 10(26): 1–49
30. Zhang L. Predicting seismic liquefaction potential of sands by optimum seeking method. Soil Dynamics and Earthquake Engineering, 1998, 17(4): 219–226
31. Hu J L, Tang X W, Qiu J N. Assessment of seismic liquefaction potential based on Bayesian network constructed from domain knowledge and history data. Soil Dynamics and Earthquake Engineering, 2016, 89(10): 49–60
32. Ahmad M, Tang X W, Qiu J N, Ahmad F. Interpretive structural modeling and MICMAC analysis for identifying and benchmarking significant factors of seismic soil liquefaction. Applied Sciences (Basel, Switzerland), 2019, 9(2): 233
33. Ahmad M, Tang X W, Qiu J N, Ahmad F. Evaluating seismic soil liquefaction potential using bayesian belief network and C4. 5 decision tree approaches. Applied Sciences (Basel, Switzerland), 2019, 9(20): 4226
34. Ahmad M, Tang X, Qiu J, Gu W, Ahmad F. A hybrid approach for evaluating CPT-based seismic soil liquefaction potential using Bayesian belief networks. Journal of Central South University, 2020, 27(2): 500–516
35. Li L, Wang J, Leung H, Jiang C. Assessment of catastrophic risk using Bayesian network constructed from domain knowledge and spatial data. Risk Analysis: An International Journal, 2010, 30(7): 1157–1175
36. Tesfamariam S, Liu Z. Seismic risk analysis using Bayesian belief networks. In: Handbook of Seismic Risk Analysis and Management of Civil Infrastructure Systems. Cambridge, UK: Woodhead Publishing Limited, 2013, 175–208
37. Witten I H, Frank E, Hall M. Data Mining: Practical Machine Learning Tools and Techniques. Burlington, MA: Elsevier, 2005
38. Bradley A P. The use of the area under the ROC curve in the evaluation of machine learning algorithms. Pattern Recognition, 1997, 30(7): 1145–1159
39. Oommen T, Baise L G, Vogel R M. Sampling bias and class imbalance in maximum-likelihood logistic regression. Mathematical Geosciences, 2011, 43(1): 99–120
40. Hamdia K M, Marino M, Zhuang X, Wriggers P, Rabczuk T. Sensitivity analysis for the mechanics of tendons and ligaments: Investigation on the effects of collagen structural properties via a multiscale modelling approach. International Journal for Numerical Methods in Biomedical Engineering, 2019, 35(8): e3209
41. Ayad F, Bekkouche A, Houmadi Y. Sensitivity analysis of soil liquefaction potential. Earth-Science Reviews, 2014, 3(1): 14
42. Pirhadi N, Tang X, Yang Q, Kang F. A new equation to evaluate liquefaction triggering using the response surface method and parametric sensitivity analysis. Sustainability, 2019, 11(1): 112
43. Cheng J, Greiner R, Kelly J, Bell D, Liu W. Learning Bayesian networks from data: An information-theory based approach. Artificial Intelligence, 2002, 137(1–2): 43–90